Journal of Renewable Materials
DOI:10.32604/jrm.2020.012488
Review

Review on Bond Properties between Wood and Fiber Reinforced Polymer

Zhen Wang[1], Haitao Li[1,2,*], Rodolfo Lorenzo[3], Ileana Corbi[4], Ottavia Corbi[4] and Changhua Fang[2]

[1]College of Civil Engineering, Nanjing Forestry University, Nanjing, 210037, China
[2]Department of Biomaterials, International Centre for Bamboo and Rattan, Beijing, 100102, China
[3]University College London, London, WC1E 6BT, UK
[4]University of Naples Federico II, Naples, 80133, Italy
[*]Corresponding Author: Haitao Li. Email: lhaitao1982@126.com
Received: 01 July 2020; Accepted: 22 July 2020

Abstract: Retrofitting of existing ancient and modern timber structures has been an important project recently. And it triggers a need of excellent strengthening methods, so does the strengthening of newly built architecture. Traditional strengthening methods have shortcomings such as high costing and destroying the aesthetic of the structure, many of which can be overcome by means of using fiber reinforced polymer (FRP) composites. However, the behavior of FRP-to-wood systems has yet to be thoroughly researched compared with their FRP-to-concrete or FRP-to-steel counterparts. As FRP retrofitting and strengthening timber structures has a promising future, better understanding of their failure modes will enable more precise designs balancing safety and cost. Three of the most common FRP-to-wood systems in the literature are discussed in this paper, namely, the externally bonded reinforcement (EBR), the near-surface mounted (NSM) and the glued-in rods (GiR) techniques. Debonding of the FRP from the substrate is one of the most common failure modes, which exhibits the significance of the interface bond between FRP laminates and wood. Hence, bond properties and behavior of FRP-to-wood composite systems are described, parameters influencing the composite action are summarized in this paper, previous works on the bond interface of FRP and timber element are reviewed and future topics are also suggested. This work can provide a reference for future research and engineering applications.

Keywords: FRP; wood; bond strength; strengthening; retrofitting

1 Introduction

Due to its outstanding properties such as high elastic modulus, high fatigue performance, high stiffness and strength-to-weight ratio and superior resistance, fiber reinforcement polymer (FRP) combining high strength fibers and a resin matrix, has been widely used in practice [1]. Its versatility has been demonstrated by a wide variety of industrial applications, particularly for strengthening of concrete structures [2–4] and steel structures [5–8]. More recently, timber structures have also been considered as an area of application. In contrast with FRP, wood as well as bamboo has been broadly utilized in construction for thousands of years and has numerous applications in structural engineering [9–12].

Although being renewable, recyclable, relatively inexpensive and architecturally attractive, wood possesses inherent defects, such as biodegrade over time and be dimensionally unstable under alternating environmental conditions.

To solve this problem, research programs focused on the reinforcement of wood beams have examined the use of FRP applied on the tension side. FRP materials have excellent mechanical properties and exhibit very good characteristics especially in relation to long-term behavior such as corrosion resistance [13,14]. FRPs have been employed either to improve flexural and shear characteristics of existing structures or to reduce the dimension of new timber structures. Three of the most common FRP-to-wood systems in the literature are: the externally bonded reinforcement (EBR), the near-surface mounted (NSM) and the glued-in rods (GiR) techniques. EBR consists of FRP laminates bonded on the surface of the timber element, which is usually used to retrofit existing timber structures. While NSM is an efficient method to strengthen newly built structures due to its greater efficiency in flexural and shear strengthening. Groove is cut near the wood surface before inserting FRP bar into it with adhesive in the NSM system. As illustrated in Fig. 1. GiR have been used in the construction engineering for decades based on steel rods, however, FRP rods have multiple advantages, such as improved mechanical properties, high resistance and increased compatible with resin and timber which point towards FRP GiR as a suitable strengthening method for wood.

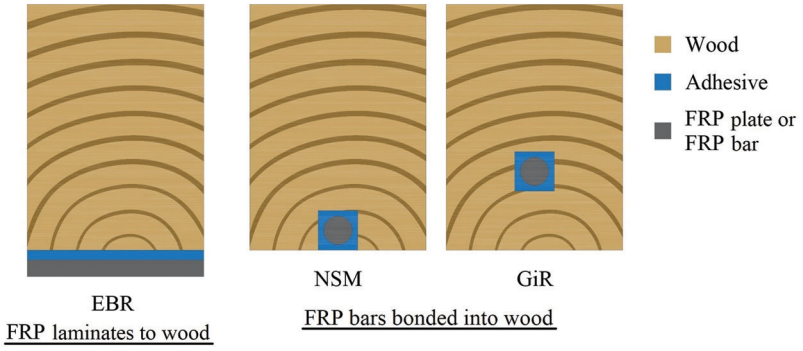

Figure 1: Different FRP-to-wood systems

Bond behavior has always been a crucial issue in strengthening techniques since it has a significant impact not only on the ultimate load-carrying capacity of the composite strengthening system but also on serviceability aspects such as deformation and crack width. Although FRP strengthening wood appears more and more frequently as a research subject in literature, the study on the bond behavior is still in its infancy as illustrated in Fig. 2.

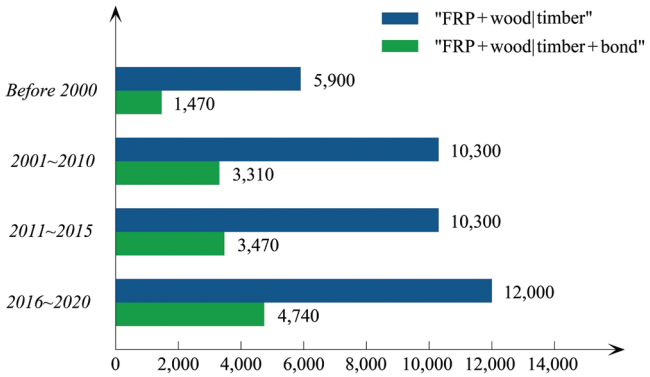

Figure 2: Number of search results for terms "FRP + wood| timber" and "FRP + wood| timber + bond" in Google Scholar

This paper presents a review on the bond properties and behavior of FRP as a strengthening alternative for timber structures including a summary of previous tests conducted in literature and the main parameters influencing the bond strength. Future research topics are also suggested.

2 Bond of FRP-to-Wood System

2.1 Bond of FRP Laminates to Wood

The feasibility of the FRP-wood bonding technique [15] such as mechanical enhancement [16–19], failure mode [20], selection of adhesive [21–23], selection of FRP [24] and effects from environmental conditions [25,26] has been covered by a number of studies in the literature. Biscaia et al. [27] revealed that the FRP-wood interfaces had the highest strength among the interfaces between FRP and three substrates: concrete, steel and wood. From all these studies, a general agreement that the FRP-to-wood is indeed an efficient approach to strengthen the wood material can be reached.

In spite of the many merits of FRP reinforcing or retrofitting structures, there are still some fundamental disadvantages in the external bonding application to structural members. Much of the success of this technique is heavily dependent on the interfacial performance between the FRP composite and the substrate. As a result, the effectiveness of the stress transfer between materials for binding reinforcement method is vital for the bonding strengthening method. In the case of concrete structures, many studies suggest that premature debonding of the FRP composite from substrate occurs [28–30]. Debonding can be defined as the single most important failure mechanism of retrofitted beams [31] that occurs at much low FRP strains before the beam reaching its ultimate strain, which directly impacts the total integrity of the structure with the subsequent outcome that the ultimate capacity and desirable ductility of the structure may not be achieved.

2.1.1 Composite Action

How well stress transmits between FRP composite and the substrate, which degree of strain can be transferred to an FRP, and how much slip occurs in the adhesive, are the keys to maintaining composite action at all stages up to failure. This is one of the most important aspects of externally strengthened wood beams that will determine the forces in each material and the overall resistance of the section. Adhesive is an important carrier for FRP bonded wood system to form effective bond and transfer shear stress and normal stress in contact interface and lap joint. The performance of the adhesive directly determines the performance of the composite. Barbero et al. [32] concluded that using structural adhesive to bond FRP sheets can ensure the effective transfer of interfacial stress. While Vahedian et al. [33] regarded FRP-to-wood width ratio (the ratio of the width of FRP to the width of wood) as crucial for effective stress transfer. The low FRP-to-wood width ratio leads to a non-uniform stress distribution across the width of wood and interfacial failure at lower load level, resulting in a higher stress in the bond at failure. Furthermore, plated length has also been identified as a desirable characteristic because shear stress transfers within the bond more uniformly as the plated length increases [34].

Raftery et al. [35] concluded the dissimilarities between the composite action are:

a) moduli of elasticity,
b) surface properties,
c) reaction to creep loading, and
d) response to moisture and to alternating environmental conditions.

2.1.2 Bond Strength Models

Several models (tabulated in Tab. 1) based on empirical relations, fracture mechanics theories or modified equation for FRP-concrete surface with many parameters calibrated with experimental data [33,36–41] have been proposed for the bond strength between FRP laminates and wood. However, there is still a lack of bond strength models of FRP-to-wood compared with FRP-to-concrete.

Table 1: Bond strength models of FRP laminates to wood

Model name	Model
Triantafillou and Deskovic Model [36]	$\tau = Ae^{\omega x} + Be^{-\omega x}$ $\omega = \sqrt{\frac{G_a}{t_a t'}\left(\frac{1}{E_f} + \frac{a}{E_w}\right)}$ $t' = t_f \frac{b_f}{b_w}$
Benedetti and Colla Model [37]	$P_u = \frac{1}{2} b_f f_{ts} \sqrt{\frac{E_f t_f}{2 f_{ts}}}$
Juvandes and Barbosa Model [38]	$P_u = P_{max} \frac{L_b}{L_e}\left(2 - \frac{L_b}{L_e}\right)$ $P_{max} = c_1 k_b k_c K_\mu b_f \sqrt{E_f t_f \tau_{max}}$ $L_e = \sqrt{\frac{E_f t_f}{c_2 \tau_{max}}}$ $k_b = 1.06 \sqrt{\frac{2 - \frac{b_f}{b_w}}{1 + \frac{b_f}{400}}} 1 \le k_b \le 1.29$
Wan Model [39]	$P_u = 0.012 \gamma_w \gamma_a b_f L_e^{0.28} \sqrt{E_f t_f}$ $\tau_{(x)} = \frac{\partial J}{\partial \delta} = A^2 B C_N e^{-Bs}(1 - e^{-Bs})$ $J = \frac{1}{2} C_N P^2$ $C_N = (1/b_f)\left\{(1/C_w) + (1/C_f) + \left[(t_w + t_f + 2t_a)^2 / 4D_w\right]\right\}$ $P = A(1 - e^{-Bs})$
Biscaia Model [40]	$\tau(s) = \begin{cases} \frac{\tau_1}{s_1} \cdot s & \text{if} \quad 0 \le s \le s_1 \\ \frac{\tau_2 - \tau_1}{s_2 - s_1} \cdot s + \frac{\tau_1 s_2 - \tau_2 s_1}{s_2 - s_1} & \text{if} \quad s_1 \le s \le s_2 \\ \tau_2 & \text{if} \quad s_2 \le s \le s_3 \\ 0 & \text{if} \quad s > s_3 \end{cases}$

Table 1 (continued).

Model name	Model
Vahedian Model [33,41]	$P_u = \gamma_w \sqrt{L_e f_{ts} E_f t_f \left(\frac{b_f}{b_w}\right)^3}$ $\tau_{(x)} = \frac{6P}{b_f L_e^2}\left(1 - \frac{x}{L_e}\right)x$ $\tau_{(max)} = \frac{3P_u}{2b_f L_e}$ $L_e = \alpha\beta(f_{ts})^{0.25}\ln(E_f t_f)$ $\beta = \frac{1.25 + \frac{b_f}{b_w}}{2\left(2.5 - \frac{b_f}{b_w}\right)}$

Note: τ is the bond stress; τ_{max} is the maximum shear stress along the bond length; P_u is the maximum load. b_f, E_f and t_f are width, elastic modulus and thickness of FRP plate or sheet, respectively. b_w, E_w and t_w are width, elastic modulus and thickness of wood block, respectively; f_{ts} is tensile strength of wood block. G_a and t_a are shear modulus and thickness of adhesive layer, respectively. L_b and L_e are the bond length and effective length, respectively. A, B and a are constants. a is a parameter relating the prestress at the bottom fiber of the beam, σ_p, to the tensile stress in the fiber composite, σ_f ($\sigma_p = -a\sigma_f$). The parameters c_1 and c_2 are obtained by experimental calibration with a value of 0.7 and 10, respectively. The factor k_b represents the anchor zone geometry that has a range of 1–1.29. The surface preparation effect is represented by the factor k_c with a range in between 0.67 and 1. The factor K_μ represents the strengthening degree which can be considered as 1. γ_w and γ_a are referred to timber sides and adhesive types, respectively, in which γ_w is equal to 0.1 and 0.08 for LVL (Laminated Veneer Lumber) and hardwood, respectively. s is corresponding slip at specific location and C_N is referred to elastic stiffness; C_w and C_f are axial stiffness coefficients of the timber prism and FRP plate, respectively; D_w is bending stiffness of the timber substrate; and P is externally applied tensile force. τ_1, τ_2 and s_1, s_2, s_3 are shown in Fig. 3, which includes four stages: elastic stage which corresponds to the first branch of the bond-slip model where slips are less than s_1; softening stage where the bond stress decays linearly once this stage begins until the slip s_2 is reached; constant stage where a uniform distribution of the bond stress can be observed and the slips are between s_2 and s_3 which designated as the ultimate slip; and debonded where no interfacial bond stress is transferred between materials once the final slip is reached. According to this model, the bond stress increases with the slips within the interface and reaches a maximum value (τ_1) when the slip is s_1. Afterwards, the interface shows a softening behavior where the bond stress decreases linearly with the interfacial slips until the interfacial slip s_2. Finally, between the interfacial slips s_2 and s_3 the bond stress remains constant. Beyond the interfacial slip s_3, the CFRP composite completely debonds from the timber substrate and therefore, the bond-slip model has no bond stresses at all. x is the distance from the free end, $x = 0$ corresponds to the free end and $x = L$ represents the loaded end.

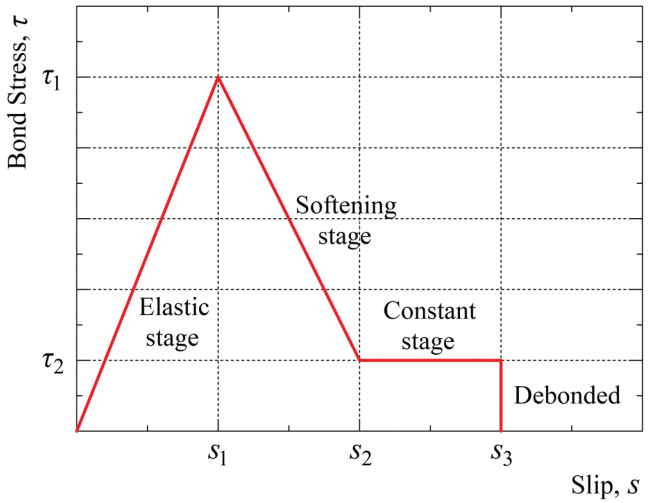

Figure 3: Bond-slip model for CFRP-to-wood interfaces [40]

2.2 Bond of FRP Bars Bonded into Wood

Since surface preparation except grooving is no longer required, the amount of installation work could be reduced in NSM or GiR compared with EBR. Moreover, debond failures which are quite common in EBR can be avoided by FRP bars reinforcement as bars are anchored into the substrate. And FRP bars are less exposed to external service environment resulting in the unchanged aesthetic of the strengthened structure and a better long-term performance [42].

Due to high mechanical properties, ease of application, a high stiffness-to-weight ratio (10- to 15-times higher than the steel) and good long-term behavior of FRP bars, the use of FRP has been encouraged as a substitute for steel. However, current research involving FRP reinforcement has concentrated on the FRP bar strengthening concrete, and the restricted data are accessible on the FRP bar reinforcing wood particularly the response of the interface bond between FRP bar and wood block. Meanwhile, design guidelines such as that provided in Eurocodes for steel bars cannot be completely mirrored for this purpose due to essential differences in surfaces deformations and mechanical properties.

The enhancement of FRP bar strengthening wood members has been proven by many researchers. Johnsson et al. [43] found that GiR reinforcement method increased the short-term flexural load-carrying capacity of glulam beams by 49%–63% on average. The reinforced beams demonstrated a moderate enhancement in ultimate moment capacity and stiffness [44,45].

According to Jahreis et al. [46], stress in the interface of FRP bar and wood is not distributed uniformly. Madhoushi et al. [47] reported that shear stress of bar/adhesive interface is much larger than the one of adhesive/wood. Raftery et al. [48] concluded that bond behavior of bonded-in FRP rod reinforcing beams can be improved by reducing the effects of stress concentrations.

Tab. 2 shows several models in the literature [46,49–52].

Table 2: Bond strength models of FRP bars bonded into wood

Model name	Model
Riberholt P Model [49]	$P_{u,v,k} = f_{ws} d \rho_k \sqrt{l_b}$ for $l_b \geq 200$mm $P_{u,v,k} = f_{wl} d \rho_k l_b$ for $l_b < 200$mm
BS ENV: 1995-2 (1997) Model [50]	$P_{u,v,k} = f_{v,k} \pi d_{equ} l_b$ $f_{v,k} = 1.2 \times 10^{-3} \times d_{equ}^{-0.2} \rho_k^{1.5}$
DIN: 1052-12 (2008) Model [51]	$P_{u,v,k} = \pi d l_b f_{v,k}$ $f_{v,k} = \begin{cases} 4.0 & \text{for} \quad l_b \leq 250\text{mm} \\ 5.245 & \text{for} \quad 250 < l_b \leq 500\text{mm} \\ 3.499 & \text{for} \quad 500 < l_b \leq 1000\text{mm} \end{cases}$ $P_{u,v,k} = \pi l_b f_{v,k} d_{equ} (1 + k_1)\ (1 + k_2)\ k$
Jahreis Model [46]	$f_{v,k} = \begin{cases} 4.0 & \text{for} \quad l_b \leq 250\text{mm} \\ 5.25 - 0.075 l_b & \text{for} \quad 250 < l_b \leq 500\text{mm} \end{cases}$ $k_1 = \dfrac{E_c A_c}{E_t A_t}$ $k_2 = \dfrac{E_a A_a}{E_t A_t}$
Yeboah Model [52]	$P_{u,mean,k} = \pi f_{v,mean} d_h l_b$ $l_b = 15 d_h$ for $l_b > 15 d_h$

Note: $P_{u,v,k}$ is the pull-out capacity; the strength parameters f_{ws} and f_{wl} are given as 520 N/mm$^{1.5}$ and 37 N/mm^2 respectively for epoxy; $d = \min [d_r, d_h]$, d_r and d_h are the diameter of rod and drilled hole, respectively; ρ_k is the characteristic density of the timber members; l_b is the bonded length of rod; $f_{v,k}$ representing the characteristic shear strength of the timber around the hole for softwoods for all angles between the rod and the fiber direction; the equivalent diameter of the rod $d_{equ} = \min [d_h, 1.25\ d_r]$; $P_{u,mean,k}$ is the mean pull-out capacity; $f_{v,mean} = 5.7$ N/mm^2; k_1 and k_2 are factors for joint stiffness; $E_c A_c$ is the stiffness of the connector; $E_t A_t$ is the stiffness of the timber; $E_a A_a$ is the stiffness of the adhesive; The parameter for stiffness of adhesive $k = 1.1$–1.2.

3 Tests the Bonded Interfaces between FRP and Wood

3.1 FRP Laminates to Wood

3.1.1 Bond Test Methods

Different bond testing methods were adopted by various researchers for different purposes of study, as illustrated in Fig. 4. They can be categorized into three types:

The Type 1 testing method involves contoured double-cantilever beam (CDCB, see Fig. 4a) bilayer specimens, which are designed by the Rayleigh-Ritz method to conduct Mode I fracture tests of bonded FRP-wood interfaces.

To conduct Mode II fracture test, three different setups of Type 2 testing method are recommended as follows. A shear-block test specimen composed of FRP and a timber block as described in ASTM D-905 is involved in the test (see Fig. 4b(i)). However, this method is only applicable to FRP plate (e.g., Barbero et al. [32]) because compression loading is applied on FRP directly. A modified double-notched test specimen shown in Fig. 4b(ii) is analogous to the one above. It consists of two timber blocks and a piece of FRP plate or sheet, where the block on the left side is fixed while load is applied to the block on the right side. Raftery et al. [35], Crews et al. [53] have adopted this kind of set up to conduct the test. As FRP is sandwiched between two timber blocks, FRP plate surface strains are difficult to monitor, not to mention the shear stress distribution and bond-slip responses. Another set up allows detailed monitoring and inspection of the failure process, due to only one possible path for debonding, as shown in Fig. 4b(iii) adopted by Wan et al. [39,54], Biscaia et al. [40] and Vahedian et al. [33]. This method is also consistent with that used in studying the bond between FRP and concrete or steel. However, it is a challenge to be sure that the alignment is maintained to minimize load eccentricity. This method may not be applicable for FRP sheets with the difficulty in gripping the sheets.

The Type 3 test method involves a piece of FRP sheet/plate attached to the tensile flange of a timber beam. The loading is applied on the beam to create a pure bending zone. This type of testing closely replicates the adhesive shear and peel stresses that are induced by flexural loads. This method consists of two cases, one in which the FRP is stuck only at the middle section of the beam (see Fig. 4c(i), Vahedian et al. [34]) and the other extends to the both ends of beam (see Fig. 4c(ii)). It is worth noting that the second case seems to be the only method when prestressed FRP laminates as external reinforcement of wood beams is encountered [36,47].

Based on the above discussions, it is recommended that the test set up illustrated in Fig. 4b(ii) be used for FRP sheets, and that in Fig. 4b(iii) be used for FRP plates to conduct Mode II fracture test in establishing the bond-slip relationship between FRP and wood in tension as surface strain can be easily monitored.

3.1.2 Failure Modes

Fig. 5 shows possible failure modes in an FRP bonded wood system including:

a) Wood crack,
b) Wood and adhesive interface failure,
c) Cohesive failure (adhesive layer failure),
d) FRP and adhesive interface failure,
e) FRP delamination (separation of some fibers from the resin matrix), or
f) FRP rupture.

The failure modes can be separated into two categories based on the duration of composite action between the materials. Failure will occur in wood or FRP, i.e., (a) or (e), (f), when composite action is maintained until the ultimate load is reached. However, when composite action is not maintained until the ultimate load is reached, premature failure results from debonding of the FRP laminates, termed

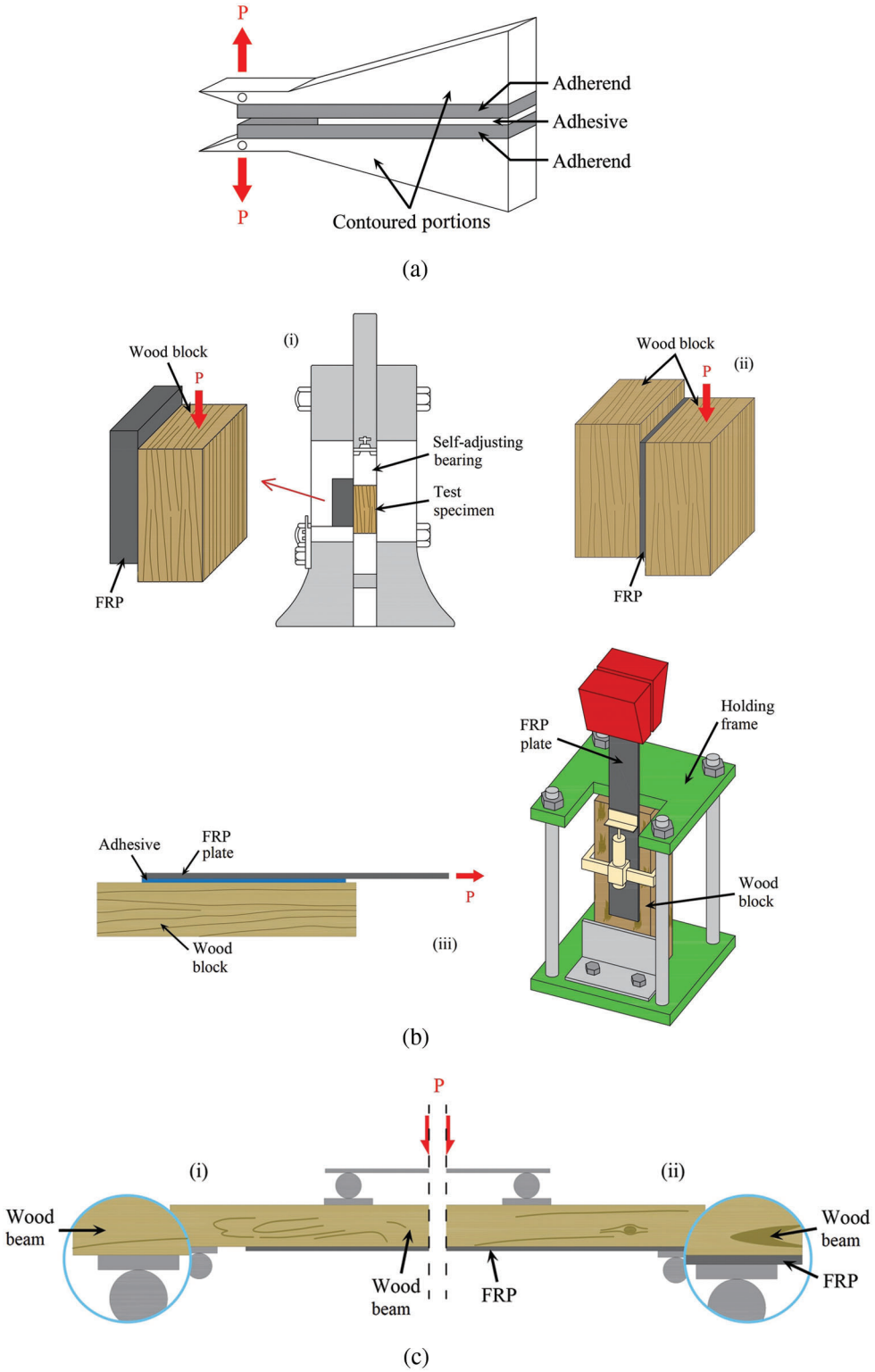

Figure 4: Schematics of testing methods to evaluate bond of FRP laminates to wood. (a) Type 1: contoured double-cantilever beam (CDCB) for Mode I fracture test [55], (b) Type 2: single-lap shear joints for Mode II fracture test: (i) shear-block test specimen and shearing tool of ASTM D-905 [32]; (ii) double-notched test specimen [35,53,56]; (iii) single-lap shear joint and shearing tool [33,39,40,54] and (c) Type 3: wood beam test: (i) FRP laminate is terminated far from the supports [34]; (ii) FRP laminate extends to the supports [36,57,58]

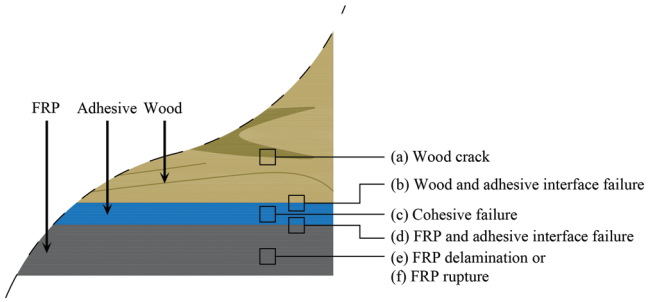

Figure 5: Schematic view of failure modes

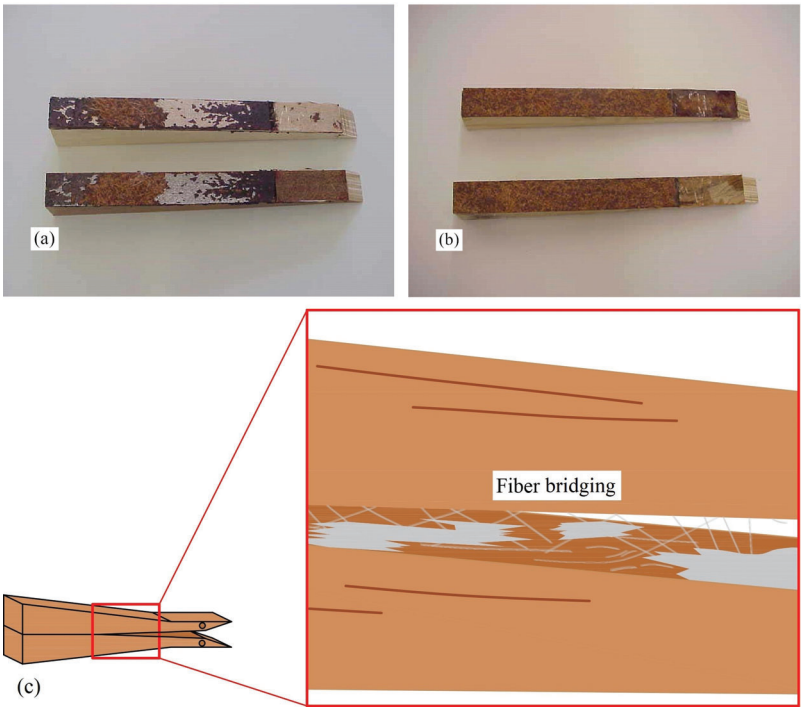

Figure 6: Failure modes of Type 1 tests: (a) fractured faces for a CDCB specimen; (b) fractured faces having fiber bridging for a CDCB specimen [59]; (c) schematic view of fiber bridging

interfacial debonding ((b), (c) and (d)). Interfacial debonding is the most common mode of failure for FRP bonded wood system. It should be noted that for multi-layer FRP sheets, it is not practical to single out failure modes (c) and (d). A schematic view of failure modes is given in Fig. 5, while some examples are given in Figs. 6–8.

Observations of fracture surface of the Type 1 test specimen in Fig. 6a shows that interfacial adhesive failure was the most common failure mode. While some failure occurred within the continuous strand mat layer of the FRP accompanied by interfacial adhesive failure. In addition, substantial fiber bridging was eminent during the fracture process in several specimens. An example is shown in Fig. 6b and a schematic view of fiber bridging is shown in Fig. 6c [55,59].

Compared to failure modes in Mode I fracture tests, those in Mode II show greater diversity [33,39,53,54]. Among all five modes shown in Fig. 7, timber-adhesive interface in timber failure is

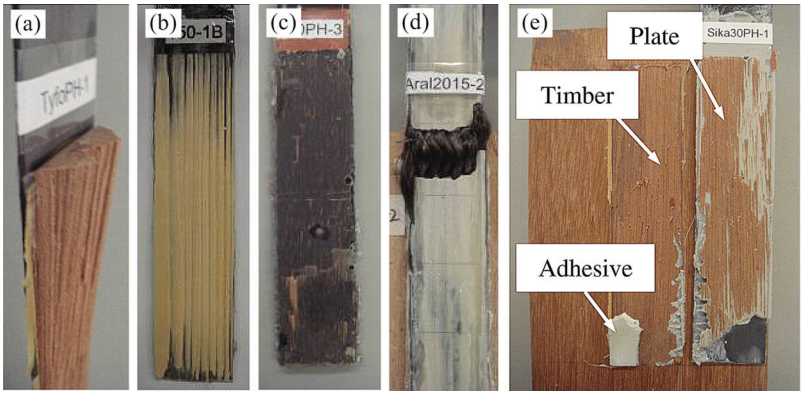

Figure 7: Failure modes of Type 2 tests: (a) wedge failure in wood; (b) timber-adhesive interface in wood; (c) wood-adhesive interface (transparent adhesive); (d) epoxy rupture; (e) adhesive-FRP interface (indicated by "adhesive") [39]

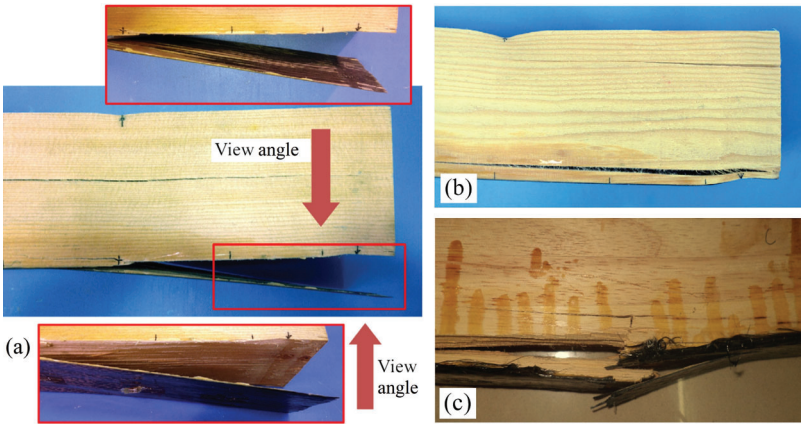

Figure 8: Failure modes of Type 3 tests: (a) ripping failure at epoxy-wood interface; (b) wood cracking [57]; (c) FRP composite sheet rupture [60]

predominantly the failure mode in FRP-to-wood Mode II fracture. The failure occurs generally at a few millimeters from the interface of the FRP and wood substrate and mainly in the wood.

Failure initiating at the interface of the FRP and timber substrate of the end of FRP laminates is found to occur frequently in wood beams strengthened using FRP. Such failure is characterized by the formation of an oblique crack from the soffit of the beam to the level of natural texture of wood. Cracking proceeds along the level of the tensile flange until the FRP laminate is completely separated from the wood beam. This failure mode is referred to as ripping or end peel failure (see Fig. 8) which is found to occur frequently in beams where the FRP laminate is terminated far from the supports.

3.2 FRP Bars Bonded into Wood

3.2.1 Bond Test Methods

There are several test configurations seen in the literature that can be used to evaluate pull-out capacity of a bar glued into timber. Pull-pull, pull-push, pull-pile foundation, pull-beam and pull-bending have been conducted mostly. While they can also be classified as: single-shear test, double-shear test and beam test. The schematics of most common setups are shown in Fig. 9. It needs to be pointed out that this figure shows the GiR specimens, which can be replaced with NSM specimens. Beam pull-out tests (BPT, shown

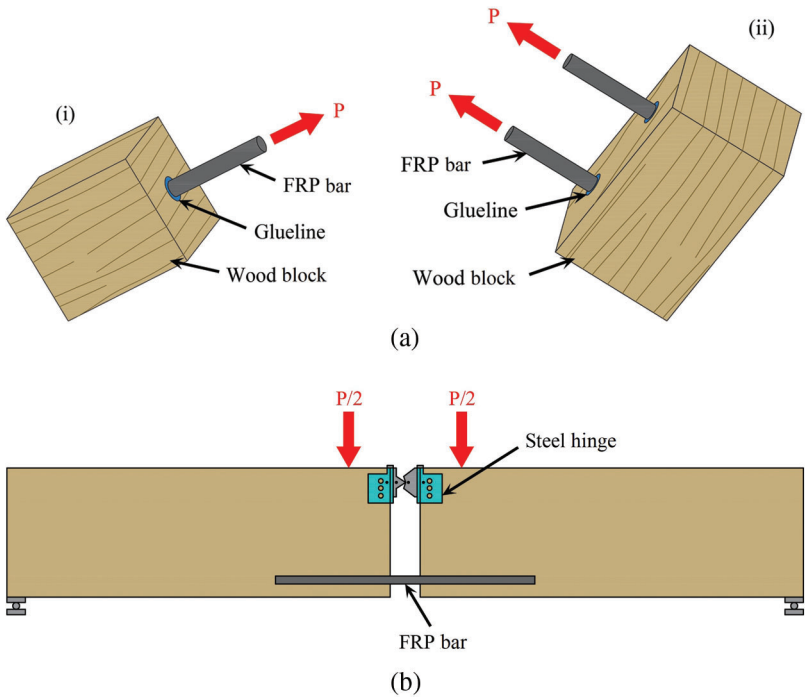

Figure 9: Schematics of testing methods to evaluate bond of FRP bars bonded into wood. (a) DPT: (i) single-shear test [46,47,63,64,67]; (ii) double-shear test [52,65,66], (b) BPT [68–70]

in Fig. 9b) are more likely to represent the actual conditions than the direct pull-out tests (DPT, shown in Fig. 9a), but significant limitations are also present for this setup as it cannot be applied to other sections directly [61]. It is worth noting that numerical and experimental investigations have demonstrated that different test setups can produce different results, and small variations in setup may have significant effects [62].

3.2.2 Failure Modes

Tab. 3 is a summary table for failure modes of FRP bars bonded into wood in the literature [47,64–66,68–70], which includes both NSM and GiR specimens and both test methods: DPT and BPT. Among all the modes, wood shear and adhesive failure have been observed in both cases. Whilst, both NSM and GiR have their exclusive failure modes: FRP bar tensile failure for NSM specimen and wood splitting for GiR specimen.

Lee et al.'s [65] concuded that NSM specimens showed the phenomenon of tensile fracture of epoxy which was different from debonding failure of EBR specimens in DPT, and the failure pattern was same each other regardless of the bonded length, width and depth. Corradi et al. [66] reported three failure modes of NSM specimens shown in Fig. 10a in DPT, which were: bar pull-out (i.e., CFRP bar/adhesive failure), timber shear failure and CFRP bar tensile failure (appeared in NSM specimens only). More bond failures were observed in Sena-Cruz et al.'s [69] beam pull-out tests because not only shear but also bending force were applied to FRP-to-wood system.

For GiR specimens, adhesive and wood shear failure are prevalent as much as NSM specimens. However, wood splitting is only observed in GiR specimen as one end of the FRP bar is completely embedded in the wood. Fig. 11 shows the failure modes of GiR specimens according to O'Neill et al. [68]. O'Neill et al. [70] also carried out tests to assess the bond strength of FRP-wood in GiR beam. They found that 64% of specimens were failing in wood shear and concluded it as wood is the weakest element in the system. Splitting of wood also appeared and the length of the splitting is equal to the bond length of FRP bar.

Table 3: Failure modes of FRP bars bonded into wood (including NSM and GiR specimens)

	DPT	BPT
NSM	Wood shear failure; Adhesive failure; *FRP bar tensile failure*	Wood shear failure; Adhesive failure
GiR	Wood shear failure; *Wood splitting*; Adhesive failure	Wood shear failure; *Wood splitting*

Note: Text marked in italics are failure modes exclusive to NSM or GiR specimen.

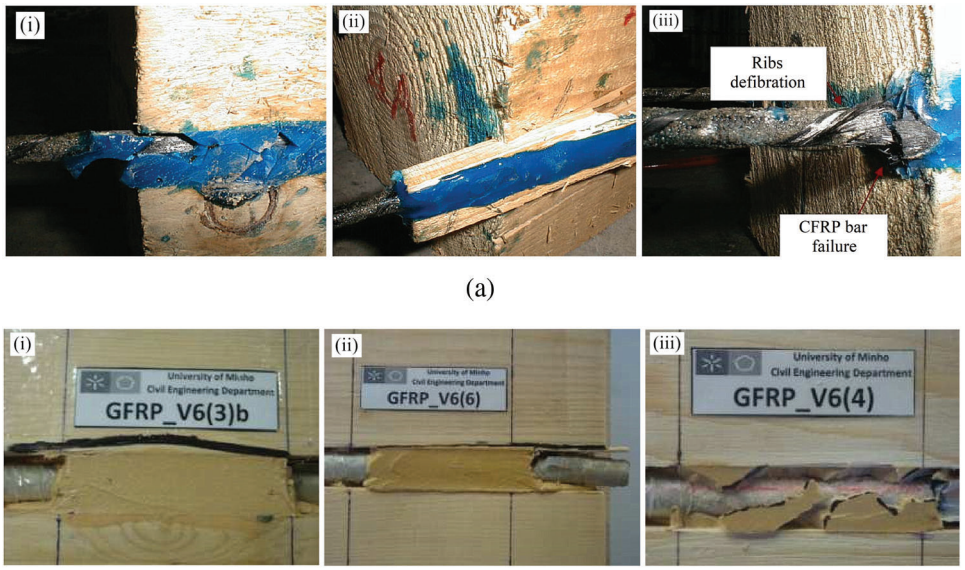

Figure 10: Typical failure modes of NSM specimens. (a) Failure modes of DPT: (i) bar pull-out; (ii) timber shear failure; (iii) CFRP bar tensile failure [66] and (b) Failure modes of BPT: (i) glulam shear failure; (ii) glulam/adhesive interfacial sliding; (iii) FRP/adhesive interfacial sliding & adhesive splitting [69]

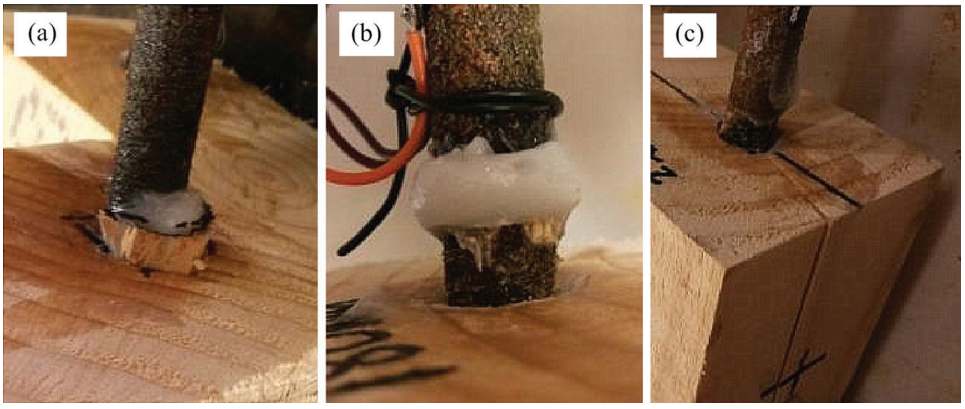

Figure 11: Typical failure modes of GiR specimens: (a) shear in timber; (b) bar/adhesive failure; (c) timber splitting [68]

4 Parameters Influencing Bond Strength of FRP Laminates to Wood

4.1 Wood

In Vahedian et al.'s [71] research, a higher ultimate load was recorded for FRP-timber joints made from hardwood when compared with the joints made from LVL (usually using softwood species), with an increase of 8%. Higher tensile strength of the hardwood species leads to the improvement of the bond strength. And they also found that specimens made from LVL exhibited a degree of ductile behavior, failing gradually; while joints made from hardwood exhibited brittle behavior, failing suddenly. According to Wan et al. [39], all softwood joints failed predominantly in the timber, whereas the hardwood joints exhibited failure at different interfacial positions.

Wan et al. [54] experimentally evaluated the influence of different bond surfaces of wood on the interfacial strength. Sides A and B bonded FRP specimens illustrated in Fig. 12 were designed for tests, where the annual growth rings of wood were predominantly oriented parallel to the FRP plate of Side A specimen and perpendicular to the FRP plate of Side B specimen. The weakness of FRP-wood interfacial strength for Side B specimen has been demonstrated by the debonded surface of the FRP plate in which a large portion was covered in thick wood of up to 5 mm thickness (see Fig. 7a), while the wood attached to the plate of Side A specimen was considerably less. Furthermore, the effect of pith was only eminent in the Side A specimen. Reasons may be due that the radius of the growth rings in the immediate vicinity of the pith is smallest leading to more perpendicular intersections of the FRP plate and growth rings, and the denser older wood next to the pith contributes to higher interfacial strength which was particularly evident in the large range of the results for the 120 mm and 180 mm bond length specimens.

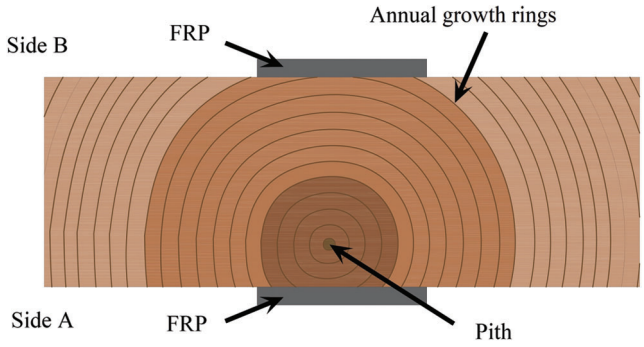

Figure 12: Wood growth characteristics and FRP bonding schemes of Wan et al.'s [54] research

The effect of grain orientation of the substrate has also been assessed by Subhani et al. [72]. Three groups of specimens were used to test the bond between CFRP and LVL by applying CFRP composite parallel (Group 1 and 2) or perpendicular (Group 3) to the grain on laminate face (Group 1) or the grain face (Groups 2 and 3) of LVL. The schematic view of Groups 1–3 is posted in Fig. 13. The result shows that the maximum shear strength of Group 1 and 2 are quite similar expect that Group 1 was more ductile than Group 2. However, Group 3 showed a poor bond performance compared to Groups 1 and 2 due to the weak material properties of timber perpendicular to the grain.

Therefore, it can be concluded that surface characteristics of wood prism been used need to be known for determining the bond strength when FRP is bonded to wood.

4.2 Moisture Content

The moisture content of wood affects the physical and mechanical properties of wood as well as the material itself, which also affects the interface bonding performance of FRP-to-wood. Water adsorbed by

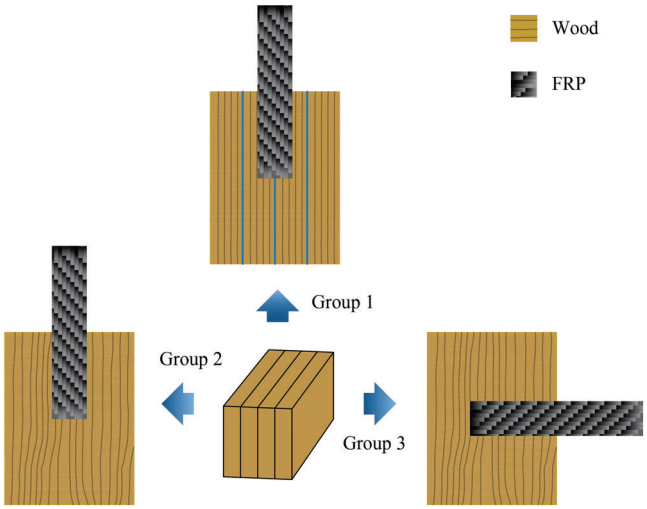

Figure 13: Schematic view of Groups 1–3 in Subhani et al.'s [72] research

wood exists between the microfibril in the cell wall and acts as a lubricant, allowing certain slippage or relative displacement between the microfibril. When the water is lost, the microfibril draw closer to each other and attract to each other, making a strong frictional resistance to the sliding displacement. Therefore, when the moisture content is lower than the fiber saturation point, the wood strength decreases with the increase of moisture content. And the strength reaches the minimum value as soon as the moisture content arrives at the fiber saturation point. As moisture content is higher than the fiber saturation point, the free water content increases while the strength remains stable. The research results in the literature show that the interfacial bonding property of the dry case for FRP sheets and wood substrate is better than that of the wet case under the same condition. Barbero et al. [32] concluded that using structural adhesive to bond FRP sheets could ensure the effective transfer of interfacial shear force, but the moisture content had a substantial adverse effect on the interfacial bonding strength. The interface shear stress of the wet FRP-wood specimen was only 43% of that of the dry one, and the shear strength of the wet specimen was about 53% of that of the dry specimen. The results also showed that due to the influence of moisture content, the strain caused by the mismatch between FRP and wood layers could be predicted by the finite element model. The swelling coefficient of wood was also determined, and the relationship between moisture content and strain of wood in the tangential and radial direction was established, which is expressed as follows:

$$\varepsilon_T = 0.0025374(MC) - 0.0285142 \tag{1}$$

$$\varepsilon_R = 0.001766(MC) - 0.017936 \tag{2}$$

where, MC is the moisture content.

Another research has been conducted by Zhou et al. [57] through performing experimental tests and molecular dynamics simulations to investigate the effect of moisture on the fracture behavior and the mechanical properties of FRP-to-wood composite. The interface fracture in moisture conditioned samples implied the weakening of the epoxy-wood interface. By performing molecular dynamics simulations, the adhesion energy of cellulose and epoxy was measured under dry and wet conditions. It is observed that water molecules diffused within the bilayer connections and led to significant decrease in adhesion energy. The adhesion energy in wet case dropped to one third of that in dry case. The findings revealed

that the bond strength between epoxy and wood decreased with moisture conditioning and the mechanical performance of FRP-reinforced wood would be significantly degraded.

4.3 FRP Gluing

4.3.1 FRP Types

Nadir et al. [60] carried out a block shear test of GFRP- and CFRP-wood specimens and reported a shear strength of 5.61 MPa and 5.52 MPa, respectively. They also experimentally tested the performance of strengthened laminated beam. For strengthened laminated wood specimens with single layer and two layers of GFRP or single layer of CFRP composite sheets, all specimens showed flexural failure occurring in the outermost wood lamination on the tension side of the beam prior to the rupture of FRP composite sheet. While in one specimen strengthened with two layered CFRP composite sheets, FRP composite sheet from the adjacent wood lamination debonded with traces of wood right after the crack occurring in the outermost wood lamination on the tensile flange of the beam. Sliding failure occurred between timber laminae accompanied by the delamination in CFRP sheet at some places in other specimens. It seems like FRP has a negligible effect on the bond strength or the failure mode of the joint on the basis of Nadir et al.'s research [60], whereas more studies are needed to confirmed it.

According to the SEM (scanning electron microscope) images of fracture surface shown in Fig. 14, the aramid fibers are not as well immersed in epoxy matrix as basalt and carbon fibers are [73]. Future researches are required to investigate whether or how fibers immersion would impact the bond performance of FRP-to-wood joint.

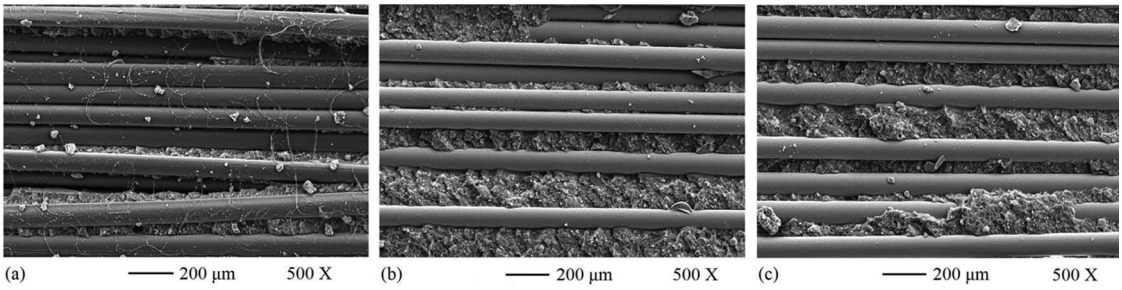

Figure 14: Microstructure characterization of (a) AFRP, (b) BFRP and (c) CFRP at failure surface [73]

4.3.2 FRP Stiffness

Biscaia et al. [40] concluded that the performance of FRP-to-wood interface is affected by the stiffness of the FRP composite. With the increase of the CFRP stiffness, the maximum load increased, and the plateaux observed in the load-slip curves decreased which is because the effective bond region was extended to satisfy the demand of the interface strength. However, if there is not enough bond region to meet the demand, the debonding happens with the increase of FRP stiffness.

4.3.3 Plate Thickness

In addition to the mechanical properties of FRP materials, the thickness, width and length of FRP plate will also affect the bond of the joint. Wan et al. [39] found that joints strengthened with pultruded plates (i.e., CFRP plates) experienced higher strengths than joints strengthened with wet layup plates (i.e., carbon sheets). One reason can be highlighted that pultruded plates are much thicker, although plate efficiencies were generally higher for sheets. Vahedian et al. [33] revealed that the brittle failure was more evident in the joints strengthened with two layers of FRP composite compared to single layer, which can be attributed to the ineffective gluing of FRP.

4.3.4 Plate Width

Plate width has been proven to have significantly impacts on the bond strength by results from the tests with different bond widths, namely, 35 mm, 45 mm, and 55 mm [33]. As FRP-to-wood width ratio increase, the interfacial bond strength of the joint increased and maximum shear stress decreased [41]. This finding is consistent with the FRP-to-concrete one in the literature [74–76]. Furthermore, the local slip at the same level of applied load decreased with width ratio increasing. One reason may be due that when the width ratio is low, the force transferred from FRP to wood results in a non-uniform of stress distribution across the width of wood, thus causing premature bond failure. And a low width ratio may lead to a high level of stress at failure, direct stress from the bonded zone of the substrate to the unbonded zone. These findings are in agreements with the previous researches conducted by Xu et al. [76] and Hollaway [77].

4.3.5 Plate Length

It was also observed by Vahedian et al. [34] that with the increase of the plated length, the ultimate bending strength increases, and conversely mid-span defection of wood beam decreases, signifying that the reinforcement leads to higher stiffness values. A noticeable decrease in shear stress at failure was obtained, too. This enhancement provides improved behavior at failure leading a more ductile collapse. That is because, shear stress transfers within the bond more uniformly and the strengthened wood beam will not collapse completely since FRP prevents crack opening and restricts local rupture.

Nevertheless, many experimental studies [31,78,79] and fracture mechanics analyses [80,81] have confirmed that extending the bond length beyond a certain length will not contribute to a better mechanical behavior of the joints where there is no increase in the bond strength. The certain length is called effective bond length.

4.3.6 Conclusion

In conclusion, FRP affects the performance of the joint superficially since the strength or stiffness of FRP materials can easily satisfy the demand of the interface performance usually, it is still the bonding that plays the decisive role. The gluing region should be large enough to avoid ineffective gluing, otherwise the reinforcing effect can be quite limited.

4.4 Prestressing

In many cases, the load-carrying capacity of the FRP is not reached as failure occurs in the wood component when FRP is in a slack state. Prestressing the FRP plate is a solution to this situation. By the means of applying a tensile force to the FRP plate prior to bonding, the prestressing force can induce compressive stresses in the flange of wood beam to offset against the tensile stresses aroused by the loads.

The effect of prestressing the FRP laminates on beam behavior was investigated by Triantafillou et al. [36], Brunner et al. [58]. Prestressing the FRP significantly improved the strength and stiffness compared to the non-stressed sheet.

Although prestressing is tested to be a good strategy to improve the properties of the composite, the premature failure of the prestressed beam caused by delamination of the laminate should be noticed.

4.5 Surface Preparation

The wood surface and FRP surface should be pretreated to roughen the surface and achieve a better combination of the composite before the FRP is pasted on the substrate (e.g., Barbero et al. [32], the FRP composite and the wood were hand sanded and wiped or air-cleaned to make the surface free from dirt and other impurities prior to bonding). Surface preparation is one of the most important processes in the whole process of reinforcement. Because the bonding is mainly based on the adhesion of the adhesive to

the wood surface and the FRP surface, the surface preparation of the material may be the main factor to determine the bonding strength and durability of the interface.

There are two different factors of surface preparation, one is the use of coupling agent or not, the other is the roughness of the surface.

Two completely different coupling agents, HMR (methyl benzodiazepines) and RF (resorcinol formaldehyde) were used for wood surface preparation by Davalos et al. [82]. The results showed that the application of HMR can effectively reduce the delamination rate of FRP-wood composite, and significantly improve the bond strength in wet-dry cycling environment as well. Superior performance of HMR has also been proven by Vick et al. [83,84] carrying out an experimental study on the bond performance between three types of adhesive and five wood species.

A comparative study on surface roughness has been conducted by Lyons et al. [85]. The wood surface was polished with sandpaper of 100-grit. It was found that the roughness and smoothness of the surface had little influence on the bond strength between FRP and wood.

4.6 Adhesive

Adhesive is an important carrier to form effective bond and transmit shear and normal stress between the contact interface of FRP-to-wood system. The performance of the adhesive directly determines the performance of the composite. Factors such as the service environment of the joint, the rigidity or flexibility of the materials, and surface conditions of the members should be taken into consideration when selecting adhesive.

The epoxy adhesive has been confirmed to be more applicable than traditional formaldehyde-based adhesive for improving the bonding performance of FRP-wood interface [32,86–89]. Raftery et al. [56] pointed out that the epoxy adhesive studied in the experimental program was considered the most suitable adhesive for the FRP-wood interface due to the excellent quality bonds under ambient conditions. Gardner et al. [90] carried out a test to evaluate the performance of three adhesives, namely RF, epoxy resin and emulsion polymer isocyanate and concluded that all three adhesives behaved well in a dry environment performance, but only the RF still had a good performance in the wet or wet-dry cycling environment.

How to apply adhesive is the crux of the bond. Although it seems to be impossible to obtain a uniform adhesive thickness as recommended by the manufacturer due to the unevenness of the composite surfaces, complete coverage on the surfaces can be ensured by forcing excess adhesive out at the sides of the composite.

Considering linear elastic fracture mechanics (LEFM), Custódio et al. [91] reported that the interfacial brittle fracture energy G_f can be determined for a given adhesive layer thickness t_a based on Eq. (3):

$$G_f = \frac{\tau_v^2 t_a}{2G_a} \tag{3}$$

where τ_v and G_a are the adhesive shear resistance and the adhesive shear modulus, respectively.

4.7 Temperature

Zhou et al. [73] concluded that the exposure temperature changed the failure modes of FRP-wood systems as the microstructure of both wood and FRP has been affected by temperature (Figs. 15a and 15b), and the wood deteriorated more rapidly than the interface with the increasing of temperature. The failure mode of the BFRP joint shifted from a mix of adhesive/cohesive failure at interface between FRP and wood at ambient temperature to cohesive failure at wood at elevated temperature. Meanwhile, the

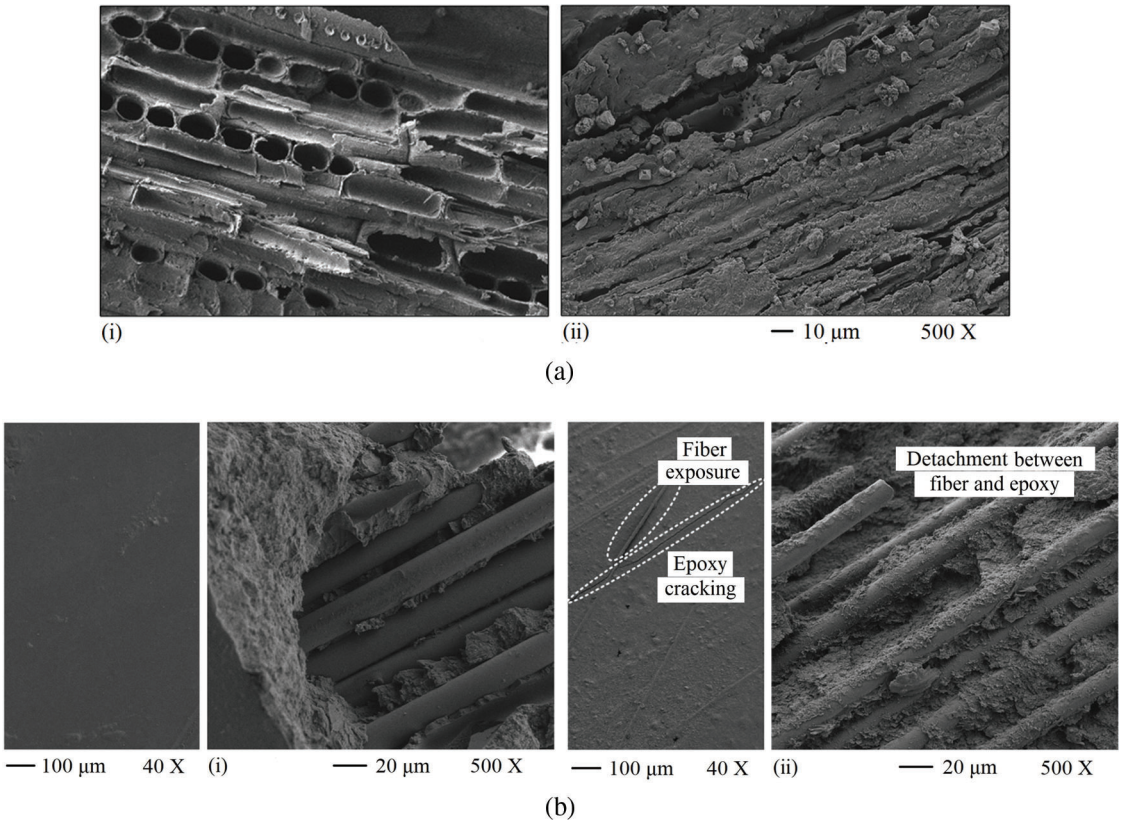

Figure 15: Microstructure characterization of wood and FRP at ambient temperature 25°C and elevated temperature of 210°C [73]. (a) Microstructure characterization of wood at failure surface at (i) ambient temperature and (ii) elevated temperature and (b) Microstructure characterization of FRP at failure surface at (i) ambient temperature and (ii) elevated temperature

interfacial fracture energy of the joint was reduced by elevated temperatures. The equations proposed by Vahedian et al. [41] (in Tab. 1) were modified via relating the effect of temperature to the coefficient α in Zhou et al.'s [73] research, and α:

$$\alpha = \pi \times \ln T, \quad 25 \leq T \leq 210 \tag{4}$$

4.8 Preservative Treatment

Some oil preservatives such as coal tar and creosote are almost inert to wood. And it does not affect the wood strength because chemical reaction will not occur in the wood after the injection. On the other hand, water-borne preservatives can enhance the compressive strength and hardness and weaken impact strength slightly with prescriptive concentration. Although the wood preservative itself has no significant effect on the wood strength when the preservative is injected into the wood, the wood strength may be significantly reduced if the temperature, pressure and other variables are not appropriate. In particular, when the pressure infusion method is adopted, the wood strength will be substantially weakened if the high temperature and high-pressure treatment is maintained for a long time.

Studies have shown that preservative treatment has complex effects on the longitudinal elastic modulus, longitudinal tensile properties and interlaminar shear properties of materials. Tascioglu et al. [92] studied the adverse effect of preservative on interface bonding performance by accelerated cyclic exposure test. The

results showed that the interfacial bonding property of preservative treatment prior to reinforcement is obviously inferior to that of preservative treatment after reinforcement. Tascioglu et al. [92] also found that brown rot fungus and white rot fungus commonly existing in wood could grow in CFRP sheet as well. The deterioration of the interfacial bonding performance due to wood-rot fungi can be detected by non-destructive technologies such as interlayer shear test and ultrasonic and scanning electron microscope.

5 Parameters Influencing Bond Strength of FRP Bars Bonded into Wood

5.1 Embedded Length

For NSM specimens, the failure load increased as embedded length increased, so well as loaded end slip. While bond stress showed a decreasing trend with increasing embedded length [66,69]. The same results were obtained from GiR specimens by O'Neill et al. [70]. However, Yeboah et al. [61] revealed that interfacial stress is in relation to the direction of the wood fibers with respect to the longitudinal axis of the joint. As the bonded length increased, GiR specimens loaded perpendicular to the grain increased in interfacial stress, while the case loaded parallel to the grain went the other way.

5.2 Groove Depth

Groove depth (the difference between the embedded length and groove depth is illustrated in Fig. 16) is another factor that influences the bond strength of NSM specimens. It has a benefit for bond strength with groove deeper, particularly when the bond length is large [69].

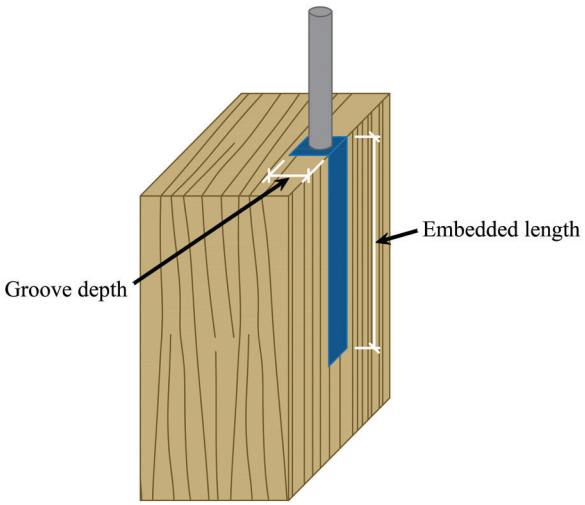

Figure 16: Schematic view of embedded length and groove depth

5.3 FRP Bar Surface

Both NSM and GiR specimens can achieve a better bond performance with a rougher surface of FRP bar because adhesive can penetrate the surface more easily [64,69]. Two different bars used in Sena-Cruz et al.'s [69] research can be seen in Fig. 17.

5.4 Adhesive and Glue-Line Thickness

The bonded strength of the GiR specimen used with poly-urethane adhesive was 2.9–4.0 times greater than the one used with resorcinol adhesive in the tests conducted by Lee et al. [93]. They also pointed out that the bond performance in the case of the glue-line thickness of 2 mm improved by 17%–29% in comparison to the case when the glue-line thickness was 1 mm. Harvey et al. [64] argued that failure load of GiR specimen

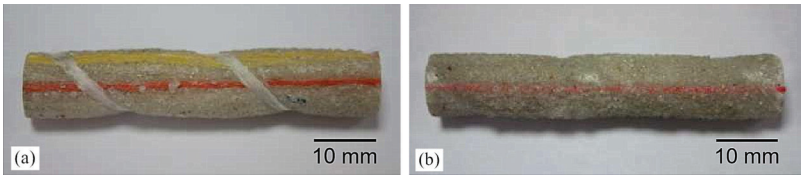

Figure 17: FRP bars used in Sena-Cruz et al.'s [69] research: (a) rough surface; (b) smooth surface

showed an upward trend with increasing glue-line thickness, which seemed to have no effect on interfacial shear stress though.

5.5 Wood Types

Lee et al. [65] and Madhoushi et al. [47] confirmed that different wood types (e.g., laminated veneer lumber, glulam and pine) can result in different bond performance of NSM or GiR specimens.

5.6 Direction of the Wood Grain with Respect to the Longitudinal Axis of the Joint

As discussed above, the direction of the wood grain with respect to the longitudinal axis of the joint has impact on the interfacial stress. Moreover, the stress-slip behavior of GiR specimen loaded perpendicular to the grain exhibited more ductile than the corresponding one parallel to the grain [60]. De Lorenzis et al. [94] pointed out that the bond strength is higher for the joints with rods perpendicular to the grain than for rods parallel to the grain, and splitting bond failure is more critical for rods parallel to the grain. The splitting bond stress of specimen loaded parallel to the grain is:

$$\tau_{\text{split}}=\frac{2r(1+r)}{2r^2+2r+1}f_{\text{u,t}} \tag{5}$$

and the splitting bond stress of specimen loaded perpendicular to the grain is:

$$\tau_{\text{split}}=1.361f_{\text{u,t}} \tag{6}$$

where $r = c/d_{\text{b}}$, c is the minimum radius of the calculation model when specimen is loaded parallel to the grain, d_{b} is the nominal diameter of the bar, $f_{\text{u,t}}$ is the tensile strength of wood in the transverse direction.

6 Other Parameters Influencing Bond Strength of FRP to Wood

Though many parameters influencing bond strength of FRP to wood have been discussed, there is still a lack of researches on other parameters. Therefore, further studies are required for this area. Fig. 18 presents a list of parameters affecting the mechanical behavior of FRP-to-wood joint which is modified from Serrano et al.'s [95] paper.

7 Summary

The behavior of FRP-to-wood systems has yet to be thoroughly researched compared with their FRP-to-concrete or FRP-to-steel counterparts. As FRP rehabilitation and strengthening of timber structures has a promising future, better understanding of their failure modes will enable more precise designs balancing safety and cost. One of the most common failure modes of wood strengthened by FRP composite is debonding of the FRP from the substrate.

Composite action between the bonded FRP and wood is very much related to the bond-slip behavior between the two materials. The currently available models for estimating bond strength of the bonded FRP to wood are based on empirical relations or fracture mechanics theories with many parameters

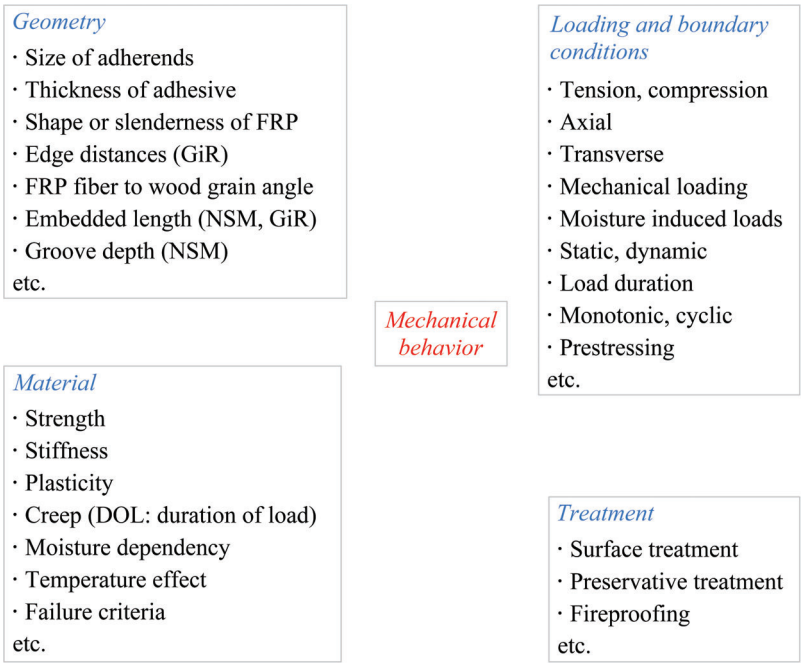

Figure 18: List of parameters affecting the mechanical behavior of FRP-to-wood joint (modified from Serrano et al.'s [95] paper)

calibrated with experimental data. The local bond-slip relationship for FRP-to-wood needs to be investigated more deeply in the future for finite element analysis.

A series of test setups for evaluating bond strength of FRP to wood have been involved in the literature. It is recommended that the test setup illustrated in Fig. 4b(ii) be used for FRP sheets, the setup in Fig. 4b(iii) for FRP plates to conduct Mode II fracture test and BPT in Fig. 9b for FRP bars to conduct NSM and GiR test in establishing the bond-slip relationship between FRP and wood.

The failure modes of wood strengthened with FRP are shown above. Although bond has a substantial impact on the performance of FRP-to-wood joints, many studies have confirmed that wood is still a weak component part in the joint. Increasing the strength of the wood material is crucial to improve the integral performance of the joint.

Parameters influencing the bond strength of FRP to wood has been discussed, while other parameters which have not been researched in literature are also suggested for future projects.

Funding Statement: The research work presented in this paper is supported by the Key Laboratory of National Forestry and Grassland Administration/Beijing for Bamboo & Rattan Science and Technology, the National Natural Science Foundation of China (Nos. 51878354 & 51308301), the Natural Science Foundation of Jiangsu Province (Nos. BK20181402 & BK20130978), Postgraduate Research &Practice Innovation Program of Jiangsu Province, Six talent peak high-level projects of Jiang-su Province (No. JZ-029), and a Project Funded by the Priority Academic Program Development of Jiangsu Higher Education Institutions. Any research results expressed in this paper are those of the writer(s) and do not necessarily reflect the views of the foundations.

Conflicts of Interests: The authors declare that they have no conflicts of interest to report regarding the present study.

References

1. Diab, H. M., Farghal, O. A. (2014). Bond strength and effective bond length of FRP sheets/plates bonded to concrete considering the type of adhesive layer. *Composites Part B: Engineering, 58,* 618–624. DOI 10.1016/j.compositesb.2013.10.075.
2. Nanni, A. (2003). North American design guidelines for concrete reinforcement and strengthening using FRP: principles, applications and unresolved issues. *Construction and Building Materials, 17(6-7),* 439–446. DOI 10.1016/S0950-0618(03)00042-4.
3. Oehlers, D., Seracino, R. (2004). *Design of FRP and steel plated RC structures: retrofitting beams and slabs for strength, stiffness and ductility.* Netherlands: Elsevier.
4. Teng, J. G., Chen, J. F., Smith, S. T., Lam, L. (2002). *FRP: strengthened RC structures*. UK: John Wiley & Sons.
5. Neale, K. W. (2000). FRPs for structural rehabilitation: a survey of recent progress. *Progress in Structural Engineering and Materials, 2(2),* 133–138.
6. Hollaway, L. C., Cadei, J. (2002). Progress in the technique of upgrading metallic structures with advanced polymer composites. *Progress in Structural Engineering and Materials, 4(2),* 131–148. DOI 10.1002/pse.112.
7. Jones, S. C., Civjan, S. A. (2003). Application of fiber reinforced polymer overlays to extend steel fatigue life. *Journal of Composites for Construction, 7(4),* 331–338. DOI 10.1061/(ASCE)1090-0268(2003)7:4(331).
8. Tavakkolizadeh, M., Saadatmanesh, H. (2003). Fatigue strength of steel girders strengthened with carbon fiber reinforced polymer patch. *Journal of Structural Engineering, 129(2),* 186–196. DOI 10.1061/(ASCE)0733-9445(2003)129:2(186).
9. Thelandersson, S., Larsen, H. J. (2003). *Timber engineering*. UK: John Wiley & Sons.
10. Li, H. T., Qiu, Z. Y., Wu, G., Wei, D. D., Lorenzo, R. et al. (2019). Compression behaviors of parallel bamboo strand lumber under static loading. *Journal of Renewable Materials, 7(7),* 583–600. DOI 10.32604/jrm.2019.07592.
11. Hong, C. K., Li, H. T., Lorenzo, R., Wu, G., Corbi, I. et al. (2019). Review on connections for original bamboo structures. *Journal of Renewable Materials, 7(8),* 713–730. DOI 10.32604/jrm.2019.07647.
12. Li, H. T., Zhang, H. Z., Qiu, Z. Y., Su, J. W., Wei, D. D. et al. (2020). Mechanical properties and stress strain relationship models for bamboo scrimber. *Journal of Renewable Materials, 8(1),* 13–27. DOI 10.32604/jrm.2020.09341.
13. Castro, P. F., Carino, N. J. (1998). Tensile and nondestructive testing of FRP bars. *Journal of Composites for Construction, 2(1),* 17–27. DOI 10.1061/(ASCE)1090-0268(1998)2:1(17).
14. Kocaoz, S., Samaranayake, V. A., Nanni, A. (2005). Tensile characterization of glass FRP bars. *Composites Part B: Engineering, 36(2),* 127–134. DOI 10.1016/j.compositesb.2004.05.004.
15. Theakston, F. H. (1965). A feasibility study for strengthening timber beams with fiberglass. *Canadian Agricultural Engineering, 7(1),* 17–19.
16. Johns, K. C., Lacroix, S. (2000). Composite reinforcement of timber in bending. *Canadian Journal of Civil Engineering, 27(5),* 899–906. DOI 10.1139/l00-017.
17. Gilfillan, J. R., Gilbert, S. G., Patrick, G. (2001). The improved performance of home grown timber glulam beams using fibre reinforcement. *Journal of the Institute of Wood Science, 15(6),* 307–317.
18. Fiorelli, J., Dias, A. A. (2003). Analysis of the strength and stiffness of timber beams reinforced with carbon fiber and glass fiber. *Materials Research, 6(2),* 193–202. DOI 10.1590/S1516-14392003000200014.
19. de Jesus, A. D., Pinto, J. M., Morais, J. J. (2012). Analysis of solid wood beams strengthened with CFRP laminates of distinct lengths. *Construction and Building Materials, 35,* 817–828. DOI 10.1016/j.conbuildmat.2012.04.124.
20. Gentile, C., Svecova, D., Rizkalla, S. H. (2002). Timber beams strengthened with GFRP bars: development and applications. *Journal of Composites for Construction, 6(1),* 11–20. DOI 10.1061/(ASCE)1090-0268(2002)6:1(11).
21. Lopez-Anido, R., Gardner, D. J., Hensley, J. L. (2000). Adhesive bonding of eastern hemlock glulam panels with E-glass/vinyl ester reinforcement. *Forest Products Journal, 50(11/12),* 43.

22. Raftery, G. M., Harte, A. M., Rodd, P. (2008). Qualification of wood adhesives for structural softwood glulam with large juvenile wood content. *Journal of the Institute of Wood Science, 18(1),* 24–34. DOI 10.1179/wsc.2008.18.1.24.
23. Raftery, G. M., Harte, A. M. (2011). Low-grade glued laminated timber reinforced with FRP plate. *Composites Part B: Engineering, 42(4),* 724–735. DOI 10.1016/j.compositesb.2011.01.029.
24. Alam, P., Ansell, M. P., Smedley, D. (2009). Mechanical repair of timber beams fractured in flexure using bonded-in reinforcements. *Composites Part B: Engineering, 40(2),* 95–106. DOI 10.1016/j.compositesb.2008.11.010.
25. Broughton, J. G., Hutchinson, A. R. (2001). Effect of timber moisture content on bonded-in rods. *Construction and Building Materials, 15(1),* 17–25. DOI 10.1016/S0950-0618(00)00066-0.
26. Raftery, G. M., Harte, A. M., Rodd, P. D. (2009). Bond quality at the FRP-wood interface using wood-laminating adhesives. *International Journal of Adhesion and Adhesives, 29(2),* 101–110. DOI 10.1016/j.ijadhadh.2008.01.006.
27. Biscaia, H. C., Chastre, C., Borba, I. S., Silva, C., Cruz, D. (2016). Experimental evaluation of bonding between CFRP laminates and different structural materials. *Journal of Composites for Construction, 20(3),* 04015070. DOI 10.1061/(ASCE)CC.1943-5614.0000631.
28. Sayed-Ahmed, E. Y., Riad, A. H., Shrive, N. G. (2004). Flexural strengthening of precast reinforced concrete bridge girders using bonded carbon fibre reinforced polymer strips or external post-tensioning. *Canadian Journal of Civil Engineering, 31(3),* 499–512. DOI 10.1139/l04-005.
29. Lu, X. Z., Teng, J. G., Ye, L. P., Jiang, J. J. (2005). Bond–slip models for FRP sheets/plates bonded to concrete. *Engineering Structures, 27(6),* 920–937. DOI 10.1016/j.engstruct.2005.01.014.
30. Khelifa, M., Celzard, A. (2014). Numerical analysis of flexural strengthening of timber beams reinforced with CFRP strips. *Composite Structures, 111,* 393–400. DOI 10.1016/j.compstruct.2014.01.011.
31. Coronado, C. A. (2006). *Characterization, modeling and size effect of concrete-epoxy interfaces (Ph.D. Thesis)*. The Pennsylvania State University, USA.
32. Barbero, E., Davalos, J., Munipalle, U. (1994). Bond strength of FRP-wood interface. *Journal of Reinforced Plastics and Composites, 13(9),* 835–854. DOI 10.1177/073168449401300905.
33. Vahedian, A., Shrestha, R., Crews, K. (2018). Bond strength model for externally bonded FRP-to-timber interface. *Composite Structures, 200,* 328–339. DOI 10.1016/j.compstruct.2018.05.152.
34. Vahedian, A., Shrestha, R., Crews, K. (2019). Experimental and analytical investigation on CFRP strengthened glulam laminated timber beams: full-scale experiments. *Composites Part B: Engineering, 164,* 377–389. DOI 10.1016/j.compositesb.2018.12.007.
35. Raftery, G. M., Harte, A. M., Rodd, P. D. (2009). Bonding of FRP materials to wood using thin epoxy gluelines. *International Journal of Adhesion and Adhesives, 29(5),* 580–588. DOI 10.1016/j.ijadhadh.2009.01.004.
36. Triantafillou, T. C., Deskovic, N. (1992). Prestressed FRP sheets as external reinforcement of wood members. *Journal of Structural Engineering, 118(5),* 1270–1284. DOI 10.1061/(ASCE)0733-9445(1992)118:5(1270).
37. Benedetti, A., Colla, C. (2010). Strengthening of old timber beams by means of externally bonded reinforcement. *World Conference on Timber Engineering* Trentino, Italy, pp. 20–24.
38. Juvandes, L. F. P., Barbosa, R. M. T. (2012). Bond analysis of timber structures strengthened with FRP systems. *Strain, 48(2),* 124–135. DOI 10.1111/j.1475-1305.2011.00804.x.
39. Wan, J., Smith, S. T., Qiao, P., Chen, F. (2014). Experimental investigation on FRP-to-timber bonded interfaces. *Journal of Composites for Construction, 18(3),* A4013006. DOI 10.1061/(ASCE)CC.1943-5614.0000418.
40. Biscaia, H. C., Cruz, D., Chastre, C. (2016). Analysis of the debonding process of CFRP-to-timber interfaces. *Construction and Building Materials, 113,* 96–112. DOI 10.1016/j.conbuildmat.2016.03.033.
41. Vahedian, A., Shrestha, R., Crews, K. (2017). Effective bond length and bond behaviour of FRP externally bonded to timber. *Construction and Building Materials, 151,* 742–754. DOI 10.1016/j.conbuildmat.2017.06.149.
42. De Lorenzis, L., Teng, J. G. (2007). Near-surface mounted FRP reinforcement: an emerging technique for strengthening structures. *Composites Part B: Engineering, 38(2),* 119–143. DOI 10.1016/j.compositesb.2006.08.003.

43. Johnsson, H., Blanksvärd, T., Carolin, A. (2007). Glulam members strengthened by carbon fibre reinforcement. *Materials and Structures, 40(1),* 47–56. DOI 10.1617/s11527-006-9119-7.
44. Micelli, F., Scialpi, V., La Tegola, A. (2005). Flexural reinforcement of glulam timber beams and joints with carbon fiber-reinforced polymer rods. *Journal of Composites for Construction, 9(4),* 337–347. DOI 10.1061/(ASCE) 1090-0268(2005)9:4(337).
45. Raftery, G., Kelly, F. (2014). Composite elements of basalt fibre rods and low grade glulam. *13th World Conference on Timber Engineering (WCTE 2014)*. Quebec City, Canda, pp. 1–10.
46. Jahreis, M., Kaestner, M., Rautenstrauch, K. (2010). Experimental and numerical analyses of glued FRP and wood by epoxy resin. *Composites, 2012,* 1–8.
47. Madhoushi, M., Ansell, M. P. (2004). Experimental study of static and fatigue strengths of pultruded GFRP rods bonded into LVL and glulam. *International Journal of Adhesion and Adhesives, 24(4),* 319–325. DOI 10.1016/j. ijadhadh.2003.07.004.
48. Raftery, G. M., Whelan, C. (2014). Low-grade glued laminated timber beams reinforced using improved arrangements of bonded-in GFRP rods. *Construction and Building Materials, 52,* 209–220. DOI 10.1016/j. conbuildmat.2013.11.044.
49. Riberholt, H. (1988). Glued bolts in glulam, proposal for CIB code international council for building research studies and documentation working commission W18. *Proceedings CIB-W18, Meeting*. Parksville, Vancouver Island, Canada, pp. 21–7-2.
50. European Committee for Standardization CEN. (2004). Eurocode 5-Design of Timber Structures-Part 2: Bridges ENV 1995-2:1997.
51. German Institute for Standardization. (2008). Design of Timber Structures-General Rules and Rules for Buildings, DIN 1052:2008-12.
52. Yeboah, D., Taylor, S., McPolin, D., Gilfillan, R. (2013). Pull-out behaviour of axially loaded basalt fibre reinforced polymer (BFRP) rods bonded perpendicular to the grain of glulam elements. *Construction and Building Materials, 38,* 962–969. DOI 10.1016/j.conbuildmat.2012.09.014.
53. Crews, K. I., Smith, S. T. (2006). Tests on FRP strengthened timber joints. *International Conference on FRP Composites in Civil Engineering*. USA: International Institute for FRP in Construction, Florida International University, pp. 677–680.
54. Wan, J., Smith, S. T., Qiao, P. Z. (2011). FRP-to-softwood joints: experimental investigation. *Advances in FRP Composites in Civil Engineering*. Berlin, Heidelberg, German: Springer, pp. 951–954.
55. Qiao, P. Z., Davalos, J. F., Trimble, B. S. (2000). Effect of moisture on fracture toughness of composite/wood bonded interfaces. *Fatigue and Fracture Mechanics,* 31, 526–544. USA: ASTM International.
56. Raftery, G. M., Harte, A. M., Rodd, P. D. (2006). Performance evaluation of adhesives and reinforcements in GFRP-wood connections. *Proceedings of the World Conference on Timber Engineering*. Portland, Oregon, USA, pp. 678–685.
57. Zhou, A., Tam, L. H., Yu, Z., Lau, D. (2015). Effect of moisture on the mechanical properties of CFRP-wood composite: an experimental and atomistic investigation. *Composites Part B: Engineering, 71,* 63–73. DOI 10.1016/j.compositesb.2014.10.051.
58. Brunner, M., Schnüriger, M. (2005). Timber beams strengthened by attaching prestressed carbon FRP laminates with a gradiented anchoring device. *Proceedings of the International Symposium on bond Behaviour of FRP in Structures,* Vol. 465, pp. 471. USA: International Institute for FRP in Construction.
59. Jia, J. (2002). *Mode-I fatigue fracture of interface for fiber-reinforced polymer composite bonded to wood (Ph.D. Thesis)*. West Virginia University, USA.
60. Nadir, Y., Nagarajan, P., Ameen, M. (2016). Flexural stiffness and strength enhancement of horizontally glued laminated wood beams with GFRP and CFRP composite sheets. *Construction and Building Materials, 112,* 547–555. DOI 10.1016/j.conbuildmat.2016.02.133.
61. Yao, J., Teng, J. G., Chen, J. F. (2005). Experimental study on FRP-to-concrete bonded joints. *Composites Part B: Engineering, 36(2),* 99–113. DOI 10.1016/j.compositesb.2004.06.001.

62. Chen, J. F., Yang, Z. J., Holt, G. D. (2001). FRP or steel plate-to-concrete bonded joints: effect of test methods on experimental bond strength. *Steel and Composite Structures, 1(2),* 231–244. DOI 10.12989/scs.2001.1.2.231.
63. Yeboah, D., Taylor, S., McPolin, D. (2016). Experimental study of interfacial stress distribution of bonded-in BFRP rod glulam joints using fibre optic sensors (FOS). *Structures, 8,* 53–62. DOI 10.1016/j.istruc.2016.08.006.
64. Harvey, K., Ansell, M. P. (2003). *Improved timber connections using bonded-in GFRP rods (Doctoral Dissertation)*. University of Bath, UK.
65. Lee, Y., Park, J., Hong, S., Kim, S. (2015). A study of bond of structural timber and carbon fiber reinforced polymer plate. *Materials Science, 21(4),* 563–567. DOI 10.5755/j01.ms.21.4.9702.
66. Corradi, M., Righetti, L., Borri, A. (2015). Bond strength of composite CFRP reinforcing bars in timber. *Materials, 8(7),* 4034–4049. DOI 10.3390/ma8074034.
67. O'Neill, C., McPolin, D., Taylor, S., Harte, A. (2014). Behaviour of basalt fibre reinforced polymer rods glued-in parallel to the grain in low-grade timber elements by Pullout-Bending tests. *Experimental Research with Timber*. Prague, Czech Republic. DOI 10.13140/2.1.4646.3365.
68. O'Neill, C., McPolin, D., Taylor, S. E., Harte, A. M. (2015). Basalt fibre reinforced polymer rods for glued connections in low grade timber. *Advanced Composites in Construction, ACIC*, UK, pp. 9–11.
69. Sena-Cruz, J., Branco, J., Jorge, M., Barros, J. A., Silva, C. et al. (2012). Bond behavior between glulam and GFRP's by pullout tests. *Composites Part B: Engineering, 43(3),* 1045–1055. DOI 10.1016/j.compositesb.2011.10.022.
70. O'Neill, C., McPolin, D. O., Taylor, S. E., Harte, A. M. (2014). Influence of embedded length on strength of BFRP rods bonded parallel to the grain in low grade timber by pullout-bending tests. *Civil Engineering Research in Ireland*. Belfast, UK. DOI 10.13140/2.1.4122.0486.
71. Vahedian, A., Shrestha, R., Crews, K. (2018). Analysis of externally bonded carbon fibre reinforced polymers sheet to timber interface. *Composite Structures, 191,* 239–250. DOI 10.1016/j.compstruct.2018.02.064.
72. Subhani, M., Globa, A., Al-Ameri, R., Moloney, J. (2017). Effect of grain orientation on the CFRP-to-LVL bond. *Composites Part B: Engineering, 129,* 187–197. DOI 10.1016/j.compositesb.2017.07.062.
73. Zhou, A., Qin, R., Chow, C. L., Lau, D. (2020). Bond integrity of aramid, basalt and carbon fiber reinforced polymer bonded wood composites at elevated temperature. *Composite Structures, 245,* 112342.
74. Chen, J. F., Pan, W. K. (2006). Three dimensional stress distribution in FRP-to-concrete bond test specimens. *Construction and Building Materials, 20(1-2),* 46–58. DOI 10.1016/j.conbuildmat.2005.06.037.
75. Ye, F., Yao, J. (2008). A 3D finite element study on the effect of FRP plate width on interfacial stress between FRP and concrete. *Bulletin of Science and Technology, 24(6),* 853–859.
76. Xu, T., He, Z. J., Tang, C. A., Zhu, W. C., Ranjith, P. G. (2015). Finite element analysis of width effect in interface debonding of FRP plate bonded to concrete. *Finite Elements in Analysis and Design, 93,* 30–41. DOI 10.1016/j.finel.2014.08.009.
77. Hollaway, L. C. (2008). Fibre-reinforced polymer (FRP) composites used in rehabilitation. In: Hollaway, L. C., Teng, J. G. (eds.), *Strengthening and Rehabilitation of Civil Infrastructures Using Fibre-Reinforced Polymer (FRP) composites*, pp. 45–82. UK: Woodhead Publishing.
78. Bizindavyi, L., Neale, K. W. (1999). Transfer lengths and bond strengths for composites bonded to concrete. *Journal of Composites for Construction, 3(4),* 153–160. DOI 10.1061/(ASCE)1090-0268(1999)3:4(153).
79. Franco, A., Royer-Carfagni, G. (2014). Effective bond length of FRP stiffeners. *International Journal of Non-Linear Mechanics, 60,* 46–57. DOI 10.1016/j.ijnonlinmec.2013.12.003.
80. Yuan, H., Wu, Z. (1999). Interfacial fracture theory in structures strengthened with composite of continuous fiber. *Proceedings of Symposium of China and Japan, Science and Technology of 21st Century, Tokyo, Japan,* 142–155.
81. Yuan, H., Wu, Z., Yoshizawa, H. (2001). Theoretical solutions on interfacial stress transfer of externally bonded steel/composite laminates. *Doboku Gakkai Ronbunshu, 2001(675),* 27–39. DOI 10.2208/jscej.2001.675_27.
82. Davalos, J. F., Qiao, P., Trimble, B. S. (2000). Fiber-reinforced composite and wood bonded interfaces: Part 1. durability and shear strength. *Journal of Composites, Technology and Research, 22(4),* 224–231.

83. Vick, C. B., Okkonen, E. A. (1997). Structurally durable epoxy bonds to aircraft woods. *Forest Products Journal, 47(3),* 71.
84. Vick, C. B. (1997). More durable epoxy bonds to wood with hydroxymethylated resorcinol coupling agent. *Adhesives Age, 40(8),* 24–29.
85. Lyons, J. S., Ahmed, M. R. (2005). Factors affecting the bond between polymer composites and wood. *Journal of Reinforced Plastics and Composites, 24(4),* 405–412. DOI 10.1177/0731684405044898.
86. Davis, G. (1997). The performance of adhesive systems for structural timbers. *International Journal of Adhesion and Adhesives, 17(3),* 247–255. DOI 10.1016/S0143-7496(97)00010-9.
87. Kim, Y., Davalos, J. F., Barbero, E. J. (1997). Delamination buckling of FRP layer in laminated wood beams. *Composite Structures, 37(3-4),* 311–320. DOI 10.1016/S0263-8223(98)80002-0.
88. Davalos, J. F., Qiao, P., Madabhusi-Raman, P., Lang, E. M. (1998). Mode I fracture toughness of fiber reinforced composite-wood bonded interface. *Journal of Composite Materials, 32(10),* 987–1013. DOI 10.1177/002199839803201005.
89. Wang, J., Qiao, P. (2003). Fracture toughness of wood–wood and wood–FRP bonded interfaces under mode-II loading. *Journal of Composite Materials, 37(10),* 875–897. DOI 10.1177/0021998303037010002.
90. Gardner, D. J., Davalos, J. F., Munipalle, U. M. (1994). Adhesive bonding of pultruded fiber-reinforced plastic to wood. *Forest Products Journal, 44(5),* 62.
91. Custódio, J., Broughton, J., Cruz, H. (2009). A review of factors influencing the durability of structural bonded timber joints. *International Journal of Adhesion and Adhesives, 29(2),* 173–185. DOI 10.1016/j.ijadhadh.2008.03.002.
92. Tascioglu, C., Goodell, B., Lopez-Anido, R. (2003). Bond durability characterization of preservative treated wood and E-glass/phenolic composite interfaces. *Composites Science and Technology, 63(7),* 979–991. DOI 10.1016/S0266-3538(03)00013-7.
93. Lee, I. H., Song, Y. J., Jung, H. J., Hong, S. I. (2015). Moment resistance performance evaluation of larch glulam joint bonded in glass fiber reinforced plastic rods. *Journal of the Korean Wood Science and Technology, 43(1),* 60–67. DOI 10.5658/WOOD.2015.43.1.60.
94. De Lorenzis, L., Scialpi, V., La Tegola, A. (2005). Analytical and experimental study on bonded-in CFRP bars in glulam timber. *Composites Part B: Engineering, 36(4),* 279–289. DOI 10.1016/j.compositesb.2004.11.005.
95. Serrano, E., Steiger, R., Lavisci, P. (2008). Glued-in rods. In: Dunky, M., Källander, B., Properzi, M., Richter, K., Van Leemput, M. (eds.), *Bonding of Timber-Core Document of the COST Action E34*, pp. 31–39. Austria: University of Natural Resources and Applied Life Sciences.